A System State aware Switched-Multichannel Protocol for Energy Harvesting CRNs

Priyadarshi Mukherjee and Swades De

***Abstract*—In this paper, we propose a novel system state aware multichannel protocol for energy harvesting cognitive radio networks (EH-CRNs). In contrast with the state-of-the-art approaches, the proposed scheme jointly accounts for the primary users traffic characteristics as well as the instantaneous channel state over a particular channel. Our analysis demonstrates that the channel state is a critical parameter for both transmission and harvesting. The proposed protocol, depending on the states of multiple channels and its data transmission versus energy harvesting priority, intelligently decides whether to enter transmission mode over a channel or harvesting mode over a potentially different channel, and the corresponding time duration. Further, exploiting the temporal correlation present in channel and also the PU traffic characteristics, the proposed protocol computes the inter-sensing interval instead of sensing the channel in every time slot, thereby enhancing the energy efficiency. Our numerical results, verified through extensive event-driven simulations, demonstrate that the proposed scheme offers an energy efficiency gain as high as 1.36 times over its nearest competitive approach.**

***Index Terms*—RF energy harvesting, cognitive radio, switched multichannel communication, fading channel, energy efficiency**

I. Background and Motivation

There has been significant growth of high throughput intensive applications in recent years. According to Ericsson [1], global Internet traffic is projected to increase by approximately nine times by year 2022. Hence it is expected that the existing wireless technologies will not be able to cater to this rising demand. On the other hand, spectrum measurement studies have shown that large portions of the licensed radio frequency (RF) spectrum are highly underutilized [2]. Cognitive radio networks (CRNs) aim to solve these problems of rising Internet traffic as well as spectrum under-utilization. CRNs allow unlicensed users to utilize the unused licensed spectrum without causing performance degradation of the licensed users.

The mode of spectrum access in CRN is broadly classified into 'white space access' (WSA) [3] and dynamic spectrum access (DSA) [4]. The spectrum availability in WSA being primarily static and pre-determined, WSA is mainly regulated by the spectrum usage database. DSA on the other hand is relatively more dynamic. As a result the unlicensed or 'secondary users' (SUs) in DSA need to have an added capability of sensing the channel availability, where the channels are owned by the licensed or 'primary users' (PUs). SUs sense the PU channels and utilize them for their own data transmission purpose whenever the PU is absent.

P. Mukherjee and S. De are with the Department of Electrical Engineering and Bharti School of Telecommunication, IIT Delhi, New Delhi, India (e-mail: {priyadarshi.mukherjee, swadesd}@ee.iitd.ac.in).

A. Related Works

In conventional DSA, an SU senses the PU channel in every time slot and performs its own communication only if the PU is absent. This not only reduces the available time for SU communication, but also results in reduced SU node lifetime. In case of intermittent PU transmissions, periodic spectrum sensing models were proposed in [5]. PU traffic dependent inter-sensing interval based scheme was proposed in [6] that aimed at maximizing the spectrum utilization. These schemes solely considered the PU traffic characteristics; dynamic channel state was not accounted in taking transmission decision.

There has been some research in the direction of channel-aware link-layer transmission schemes, though not in the CRN scenario. The study in [7] proposed sensing of channel at predetermined intervals, where data transmission takes place only if the channel state is found above a certain threshold. The authors in [8] exploited temporal correlation in channel to estimate both transmission as well as waiting windows. Adaptive modulation and coding (AMC) is a well-investigated topic in this context [9], [10]. The authors in [11] proposed AMC in context of CRNs, wherein they considered SU rate adaptation in each time slot, based on the sensing result.

Frequent spectrum sensing results in depletion of critical energy resource of the SU sensor nodes. In this context, recent research have focused on analyzing the performance of energy harvesting (EH) wireless networks [12]. EH-CRNs have received great attention in industry as well as academia as 'green' solution to the communication problem [13].

A CR node in EH-CRN is powered by harvested energy from the ambient or other sources, such as PU transmission over its own licensed channel. Harvesting tends to make the secondary system self-reliant in terms of energy, thus potentially avoiding the need for battery replacement and hence network disruption. The works in [14], [15] investigated an EH-CRN to improve both spectrum and energy efficiency. A channel selection criteria in an EH-CRN scenario was proposed in [16] that aimed at throughput maximization. Various inter-sensing interval estimation schemes were proposed in [17] for different situations, such as when PU is idle/busy or when the SU does not have sufficient energy. The authors in [17] suggested that an SU should transmit or harvest depending on whether the PU is idle or busy, as well as whether the SU is energy depleted. The study in [18] analyzed throughput of an EH-CRN based on PU activity prediction. However, the proposed prediction was based on one-slot history.

A cognitive access protocol was proposed in [19], which

was aimed at SU throughput maximization while maintaining the stability of PU's packet queue at given packet arrival and energy harvesting rates. This work considered that the SUs are plugged to a reliable power supply while the PUs are powered through a random time-varying renewable energy process. The studies in [20], [21] investigated the maximum achievable throughput. SUs were either equipped with rechargeable batteries or they harvest energy from PU's transmissions as well as the environment. The authors in [22] investigated a queuing-theoretic model for cooperative CRNs where the energy harvesting SU has a finite relay queue and a finite battery queue. A new CRN architecture based on stochastic geometric models was proposed in [23] that enabled SUs to harvest RF energy from active PUs as well as reuse their spectrum.

Overall we note that, although there have been prior studies on channel-aware link-layer transmission strategies, there is a lacuna in the existing CRN data transmission strategies. While [5] and [6] estimate inter-sensing interval based on PU traffic characteristics only, [7] and [8] exploit the channel state but in non-CRN scenarios. Channel state variation is accounted in [11], but it requires per-slot channel sensing. It is also notable that, these works did not consider the EH aspect. While the work in [19] considered SUs connected to a reliable power supply, [20]–[22] modeled the energy harvesting at SU as a Bernoulli process. Thus, channel dynamics between a SU and an active PU, over which energy harvesting is sought, has not been accounted in the prior art [14]–[18], [20]–[23]. Intuitively, if this PU-SU channel is in deep fade state, almost no power would reach the EH receiver; on the other hand if it is in very good state, a considerable fraction of power is harvested at the EH receiver. Moreover, all of these works consider a linear EH model, while the actual one is non-linear in nature [24]. Considering a similar argument for SU transmission over a PU channel, we observe that, *in scenarios where a SU has the option of selecting a certain PU channel from a pool, for EH or transmission, the PU-SU channel state plays a very important role along with the PU traffic characteristics over that channel.* Lastly, we demonstrate that it is sometimes advantageous to prioritize harvesting over transmission, even when SU has sufficient energy for transmission. Our current work is intended to explore these aspects of CRN for improved system performance.

B. Contributions

In this work, we investigate the performance of single-user switched multichannel energy harvesting cognitive radio protocols. The main contributions of the paper are as follows:

1) We propose a new energy-aware link-layer protocol for EH-CRNs. The proposed protocol intelligently decides on whether and how long to transmit data over a PU channel or harvest energy over a potentially different channel at a decision epoch, such that the delay limit on the data is not violated. Our results demonstrate that energy efficiency of the proposed protocol is about 1.36 times higher in comparison to its nearest approach.
2) Instead of SU transmitting over a channel whenever it is found idle, we propose that the selection of a channel from the pool of idle channels should be decided jointly based on the PU traffic characteristics as well as current state of the respective channels.
3) Similarly, unlike the existing works, we propose that the selection of a busy PU channel for energy harvesting should also be jointly decided by the channel state between an active PU and the SU along with the PU traffic characteristics. We also explain our claim by means of an illustration.

To the best of our knowledge, the proposed protocol that intelligently decides between the transmission mode and harvesting mode has not been explored earlier. It is important to note that the decision is based on PU traffic characteristics and the present channel state along with temporal variations, without requiring any knowledge of the underlying fading distribution. Also, the non-linear EH model considered in this work makes the proposed protocol performance more realistic and different from the existing communication protocols in EH-CRNs.

C. Paper Organization

The remaining paper is organized as follows. System model and the proposed framework are described, respectively in Sections II and III. Section IV discusses the numerical results, and the paper is concluded in Section V.

II. System Model

A single-user multichannel cognitive radio access scenario is considered, where there is a primary network of N primary users (PU) and a single secondary user (SU) pair, consisting of a SU transmitter (Tx) and a SU receiver (Rx). Besides the PUs and the SU pair, there also exists a secondary sensing terminal (SST), which has complete information of the primary network. Table I shows the list of variables used, along with the descriptions. Both primary network and SU pair are assumed to follow time-slotted synchronous communication [25], with slot duration T_s.

A. Channel Availability Characterization

The PU channels in this work are characterized using ON-OFF model. For the sake of mathematical tractability, ON and OFF period lengths are assumed to be exponentially distributed with the respective mean values μ_n and λ_n. Without any loss of generality, we assume that the time slots are small with respect to the scale of μ_n and λ_n [26], [27], which is considered to prevent the PU activity status change multiple times within a single T_s. Hence the PU activity state can be considered quasi-static within a slot duration T_s. These ON/OFF channel states are represented in terms of a discrete time Markov chain (DTMC), where the state transition probabilities are computed as:

$$\mathrm{P}_{\mathrm{ON}\rightarrow\mathrm{OFF}} \triangleq \mathrm{p}_{1,0} = \int_0^{T_s} \frac{1}{\mu_n} e^{-a/\mu_n} da = 1 - e^{-T_s/\mu_n}, \quad (1)$$

$$\mathrm{P}_{\mathrm{OFF}\rightarrow\mathrm{ON}} \triangleq \mathrm{p}_{0,1} = \int_0^{T_s} \frac{1}{\lambda_n} e^{-b/\lambda_n} db = 1 - e^{-T_s/\lambda_n}.$$

TABLE I
LIST OF VARIABLES USED AND THEIR RESPECTIVE DESCRIPTIONS

T_s	Slot duration
$\mu_n(\lambda_n)$	Average ON (OFF) period of n^{th} PU
f_D	Doppler frequency
P_p	Transmit power of active PU
P	Probing signal power of SU
P_{EH}	Harvested power at SU
M, a, b	Non-linear energy harvesting circuit parameters
h_{ps}	Complex channel gain between SU-Tx and active PU
X	Signal envelope
κ	Degree of CSI imperfection
$E(t)$	SU energy level at time t
$E_{\max}$	Maximum charging capacity of SU
$E_{\min}$	Minimum energy required for basic functionalities of SU
$D_{\max}$	Maximum delay bound
$\Theta = \{\theta_1, \cdots, \theta_N\}$	Set of all N PU channels
$\Theta_I = \{\theta_i^1, \cdots, \theta_i^{N_I}\}$	Set of N_I PU idle channels
$\Theta_B = \{\theta_b^1, \cdots, \theta_b^{N_B}\}$	Set of N_B PU idle channels
$\mathcal{M} = \{m_1, m_2, \cdots, m_{\lvert\mathcal{M}\rvert}\}$	M-QAM constellation adopted by SU
$R_j \ \forall\ j = 1, \cdots, \lvert\mathcal{M}\rvert$	Data rate of j^{th} modulation scheme from $\mathcal{M}$
$X_{T_k} \ \forall\ k = 0, \cdots, \lvert\mathcal{M} - 2\rvert$	Thresholds for channel adaptive modulation at SU-Tx
P_t	Data transmission power of SU
P_b	Bit error rate
P_{idle}	Idling power of SU
$\tau(j)$	Time required for transmission with j^{th} modulation scheme
$E_{\text{req}}(j)$	Energy required for transmission with j^{th} modulation scheme
$\theta_{i,k}^{\text{Tx}}$	Channel that SU chooses for transmission using a constellation of size m_{k+1}
θ_b^{H}	Channel that SU chooses for harvesting when it does not have sufficient energy for transmission
θ_b^{HN}	Channel that SU chooses for harvesting when $E(t) < E_{\max}$ and there is no data for transmission
θ_b^{C}	Intermediate choice of SU for energy harvesting
ϵ_0, δ	Acceptable error thresholds
D_{R}	Data rate of proposed protocol
E_{EC}	Effective energy consumption of proposed protocol
η	Energy efficiency of proposed protocol
$\varepsilon_t, \varepsilon_{\text{idle}}, \varepsilon_p, \varepsilon_s$	Per-slot transmission, idling, probing, and sensing energy
ψ	PU activity duty cycle

Accordingly the state transition matrix $\mathbb{P}$ is:

$$\mathbb{P} = \begin{bmatrix} \mathrm{p}_{0,0} & \mathrm{p}_{0,1} \\ \mathrm{p}_{1,0} & \mathrm{p}_{1,1} \end{bmatrix} = \begin{bmatrix} e^{-T_s/\lambda_n} & 1 - e^{-T_s/\lambda_n} \\ 1 - e^{-T_s/\mu_n} & e^{-T_s/\mu_n} \end{bmatrix}. \quad (2)$$

B. Secondary User Activity

When data arrives at SU for transmission, it takes a snapshot of all N channels of the primary network to identify the currently busy/idle channels. SST has the statistical information of arrival rate μ of all PUs. After obtaining this information from the SST, SU estimates the time for which a particular PU will continue to remain busy/idle given that it is currently busy/idle.

When SU identifies an idle channel, SU-Tx sends a probing signal and obtains CSI feedback through an error-free and dedicated feedback channel from SU-Rx. Since SU-Tx and SU-Rx are typically devices with similar capabilities, communicating over short range, based on the channel reciprocity of a TDD-based wireless system [28], channel gain of the uplink is considered same as that of the downlink, estimated by SU-Rx. If power of the probing signal is P, the present channel state X at time t is defined as the received signal envelope at SU-Rx, *i.e.,* $X(t) = \sqrt{Pd^{-\alpha}}|h(t)|$, where d is the SU Tx-Rx distance, α is the path-loss factor, and $h(t)$ is the circularly symmetric complex Gaussian (CSCG) channel co-efficient.

SU-Rx also sends information regarding the Doppler frequency f_D [29] to SU-Tx. $f_D \cong \frac{vf_c}{c}$, where f_c is the carrier frequency and c is the velocity of light in vacuum. Product $f_D T_s$ characterizes the rate of temporal variation of

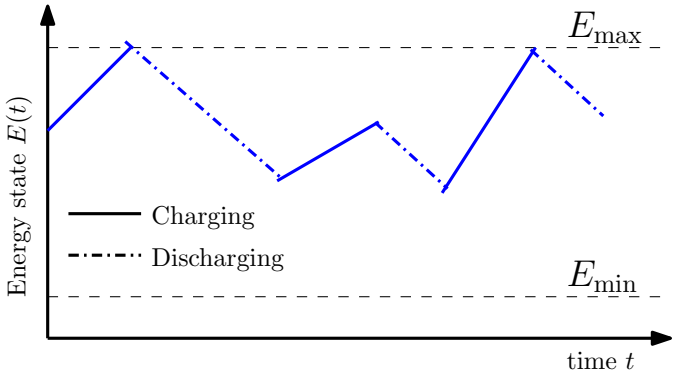

Fig. 1. Variation of SU energy level against time.

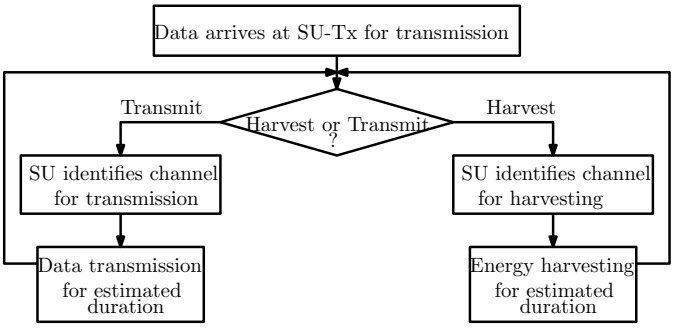

Fig. 2. Broad overview of the proposed protocol.

the channel; large value of $f_D T_s$ (> 0.2) indicates an almost independent 'fast' fading channel, whereas a small value of $f_D T_s$ (< 0.1) implies a correlated 'slow' fading channel [30]. Noting that due to the presence of scatterers, received signal at Rx can experience Doppler effect even with stationary Tx and Rx [31], the factor v (hence f_D) effectively captures the effect of mobility of Tx, Rx, or scatterers, or a combination of them. In context of this work, we have considered v in the $2-12$ kmph range, i.e., stationary Tx, Rx with mobile scatterers.

Based on these PU activity and CSI over a channel, the SU pair judges whether that particular channel is usable for data transmission, and if yes, for how long it will continue to remain so. It also decides on the modulation scheme to be employed for data transmission.

C. Energy Harvesting Model

A SU node is also equipped with an EH unit that can extract DC power from the received electromagnetic waves [32]. Based on requirement, the EH unit harvests energy from the currently active PU channels. If transmit power of the currently active PU over a channel is P_p, the power harvested at SU, P_{EH} is characterized by a non-linear model [24]:

$$P_{\text{EH}} = \frac{M(1 - e^{-aP_p d^{-\alpha}|h_{ps}|^2})}{1 + e^{-a(P_p d^{-\alpha}|h_{ps}|^2 - b)}}. \tag{3}$$

Here M is the maximum harvested power at SU when the EH circuit is saturated, h_{ps} is the complex channel gain between the active PU and the SU, and a and b are the constants that characterize the circuit parameters. Fig. 1 illustrates the variation of SU energy level $E(t)$ against time. $E_{\max}$ is the maximum charging capacity of SU and $E_{\min}$ is the minimum energy required for its basic functionalities. The charging state represents the energy harvesting state of SU, whereas the discharging state represents its energy drainage due to data transmission. Fig. 1 also depicts unequal charging and equal discharging rates. While unequal charging rate is explained by the stochastic availability of energy for harvesting, constant power of the SU for data transmission is responsible for the equal discharging rate.

A delay-constrained application is considered in this work wherein each packet at the SU-Tx needs to be transferred within a maximum delay bound of $D_{\max}$. Further, delivery of a packet content in fractions due to nonavailability of good channel over a required duration is not allowed, *i.e.,* if α bits of data in a packet are to be transmitted, all of them must be transferred simultaneously.

D. Case of Imperfect Channel Estimate

We observe from the previous sections that some knowledge of CSI is required in the proposed framework, *i.e.,* $X(t) = \sqrt{Pd^{-\alpha}}|h(t)|$. Since in realistic wireless systems perfect CSI is an overoptimistic assumption, we also study the system performance with imperfect CSI, which is modeled by a Gauss-Markov uncertainty as [33]:

$$\widehat{h} = \sqrt{1-\kappa^2}h + \kappa \mathrm{e}, \tag{4}$$

where $\mathrm{e} \sim \mathcal{CN}(0,1)$ accounts for the channel estimation errors independent of h. $\kappa \in [0,1]$ indicates the quality of instantaneous CSI, *i.e.,* $\kappa = 0$ represents perfect CSI, while $\kappa = 1$ represents having only statistical channel knowledge. Accordingly we obtain $\widehat{X}(t) = \sqrt{Pd^{-\alpha}}|\widehat{h}(t)|$. Note that $\widehat{X}(t)$ merges to $X(t)$ when $\kappa = 0$.[1]

III. Proposed Framework

Fig. 2 broadly outlines our proposed framework. The novelty of this framework lies in the 'harvest or transmit ?' block, wherein the SU opts between energy harvesting and data transmission. Here the SU 'intelligently' decides between harvesting and transmission, and also estimates its respective harvesting/transmission duration. In this section, we explore the proposed framework in details.

We define certain mathematical functions, namely, $f_I, f_B, f_{T,k}$, and $f_{H,t}$ in Table II, that are used in the proposed framework.

A. Busy and Idle Duration Estimation

Let $\Theta = \{\theta_1, \theta_2, \cdots, \theta_N\}$ denote the set of all channels, where $\theta_n = 0/1$, depending on whether the n^{th} PU is idle/active. Accordingly, $\Theta_I(\Theta_B)$ is the set of idle (busy) channels:

$$\Theta_I = \{\theta_i^1, \theta_i^2, \cdots, \theta_i^{N_I}\} \quad \text{and} \quad \Theta_B = \{\theta_b^1, \theta_b^2, \cdots, \theta_b^{N_B}\}, \tag{5}$$

[1]From now onward, the $\widehat{\ }$ sign will not be explicitly mentioned, *i.e.,* when we state $X(t) = X_0$, we will be implicitly implying $\widehat{X}(t) = X_0$.

TABLE II
FUNCTION DEFINITIONS.

f_I	Estimates time ζ_I for which a θ_i will continue to remain idle.
f_B	Estimates time ζ_B for which a θ_b will continue to be occupied a PU.
$f_{T,k}$	Estimates time $\zeta_{k,k+1}$ over a θ_i, for which X will continue to remain in $[X_{T_k}, X_{T_{k+1}})$ when $X_0 \in [X_{T_k}, X_{T_{k+1}})$
$f_{H,t}$	Estimates the amount of energy that can be harvested over a θ_b over t slots.

where $N_I + N_B = N$. Depending on whether a particular θ_n is currently idle/busy, the time for which θ_n will continue to remain idle/busy is estimated. This calculation is based on the traffic arrival characteristics of the PU that is accessing θ_n. Functions f_I and f_B estimate these values, respectively.

Definition 1. *$\zeta_I(\zeta_B)$: It is the duration (in slots) over which PU is estimated to be absent (present) in a particular θ_n, given that PU is currently absent (present) in that θ_n.*

From (2) we know that $\mathrm{p}_{1,1} = e^{-T_s/\mu_n}$. Hence for a given PU error threshold δ,

$$\mathrm{p}_{1,1}^{\zeta_B} \geq 1-\delta \implies \zeta_B \leq \frac{\mu_n}{T_s} \ln\left(\frac{1}{1-\delta}\right). \tag{6}$$

Thus it can be stated that $f_B : \Theta_B \longrightarrow \Delta_B$, where $\Delta_B = \{\zeta_B^1, \zeta_B^2, \cdots, \zeta_B^{N_B}\}$. Similarly we obtain

$$\zeta_I \leq \frac{\lambda_n}{T_s} \ln\left(\frac{1}{1-\delta}\right) \tag{7}$$

and thus, $f_I : \Theta_I \longrightarrow \Delta_I$, where $\Delta_I = \{\zeta_I^1, \zeta_I^2, \cdots, \zeta_I^{N_I}\}$.

Note that both $\zeta_I^i \ \forall\ i = 1, \cdots, N_I$ and $\zeta_B^j \ \forall\ j = 1, \cdots, N_B$ are dependent on PU traffic characteristics, *i.e.,* f_I and f_B, which map the channel availability information to ζ_I and ζ_B, respectively are PU traffic characteristics dependent functions.

B. Secondary Rate Adaptation

In this work, SU adopts a constellation set $\mathcal{M} = \{m_1, m_2, \cdots, m_{|\mathcal{M}|}\}$ with $R_j = \log_2(m_j)$ bits/symbol $\forall\ j = 1, \cdots, |\mathcal{M}|$ and m_1 signifying no transmission. The entire channel state range is divided into $|\mathcal{M}|$ regions with thresholds $X_{T_k}\ \forall\ k = 0, \cdots, |\mathcal{M}-2|$ and each region being mapped to a constellation size m_j. Bit error rate (BER) P_b, constellation size $m_j(z)$, received power $X^2(z)$, and complex channel gain $h(z)$ in the z^{th} time slot are related as [34]:

$$P_b = c_1 \exp\left(\frac{-c_2 X^2(z)}{N_0 B(j^{c_3}(z) - c_4)}\right), \tag{8}$$

where $c_p\ \forall\ p = 1,\cdots,4$ are modulation-specific constants, N_0 is the noise spectral density, and B is the channel bandwidth. For a constant transmission power P_{t} using constellation size m_j, time required (in slots) for transmission of α packets with φ bits in each packet is $\tau_{\text{req}}(j) = \left\lceil \frac{\alpha\varphi}{R_j} \right\rceil$. Accordingly, the energy required for transmission is

$$E_{\text{req}}(j) = (P_t + P_{\text{idle}})\tau_{\text{req}}(j) T_s, \tag{9}$$

where P_{idle} is the power required for circuit operation. Note that $E_{\text{req}}(j)$ is a function of the constellation size, which is not a fixed quantity.

For all the N_I empty channels, a function $f_{T,k}$ based on current channel state $X = X_0$ is defined that estimates the time $\zeta_{k,k+1}$ (in slots) over which X is expected to remain in $[X_{T_k}, X_{T_{k+1}})$, given $X_0 \in [X_{T_k}, X_{T_{k+1}})$. The entire analysis corresponding to $f_{T,k}$ is presented in the Appendix A. Also, m_{k+1} is the preferred constellation during $\zeta_{k,k+1}$.

SU chooses $\theta_{i,k}^{\text{Tx}}$ for data transmission, where $\theta_{i,k}^{\text{Tx}}$ is obtained from the optimization problem P1:

$$\text{(P1)} \quad : \underset{k,\theta_i}{\text{minimize}}\ \tau_{\text{req}}(k) \tag{10}$$

$$\begin{aligned} \text{subject to} \quad & C1 : \tau_{\text{req}}(k) \leq \min\{f_I(\theta_i), f_{T,k}(\theta_i)\}, \\ & C2 : m_{k+1} \in \mathcal{M}, \\ & C3 : \theta_i \in \Theta_I. \end{aligned}$$

$\theta_{i,k}^{\text{Tx}}$ is a particular θ_i from Θ_I which minimizes the objective in P1 using constellation m_{k+1} from $\mathcal{M}$. Note that, while $C1$ guarantees that the entire data is transmitted at one go, $C2$ guarantees that the chosen constellation is from the constellation set $\mathcal{M}$, and $C3$ guarantees $\theta_{i,k}^{\text{Tx}}$ to be one of the idle channels. Lastly, minimizing $\tau_{\text{req}}(k)$ implies that none but the best channel among all $\theta_i^a \in \Theta_I\ \forall\ a = 1, \cdots, N_I$ is chosen.

However, at times $\tau_{\text{req}}(k) \nleq \min\{f_I(\theta_i), f_{T,k}(\theta_i)\}$ may occur. In other words, time for transmission of the entire data over $\theta_{i,k}^{\text{Tx}}$ using a constellation of size m_{k+1} is less than the time for which $\theta_{i,k}^{\text{Tx}}$ is estimated to remain empty. Since transmission of a packet content in multiple patches is not allowed, the SU chooses not to transmit data during that interval. As SU avoids transmission during this interval, the delay bound now reduces to $D'_{\max}$ from $D_{\max}$, where $D'_{\max} = D_{\max} - \min\{f_I(\theta_i), f_{T,k}(\theta_i)\}$. In other words, *the delay bound becomes more and more stringent for every transmission deferral.*

Computational Complexity of P1:

To study the computation complexity of P1, it is notable that P1 is not based on Brute-force method, as described below:

1) P1 chooses a particular channel from N channels. Unlike in Brute-force method, $C3$ ensures that the search does not take place over the entire set; instead it reduces the search space to the set of N_I channels. In general, we have $N = N_I + N_B$, i.e., $N_I < N$.
2) The entire channel state range is divided into non-overlapping regions. Each region being mapped to a constellation size based on acceptable BER, $C2$ does not involve any iterative method for finding out the appropriate modulation scheme. If $X_0 \in [X_{T_k}, X_{T_{k+1}})$, modulation scheme m_{k+1} is selected accordingly from a look-up table.

3) $C1$ is evaluated on each of the N_I idle channels to find out the appropriate channel $\theta^{\text{Tx}}_{i,k}$.

Thus, it can be observed that the complexity of obtaining $\theta^{\text{Tx}}_{i,k}$ from P1 is $\mathcal{O}(N_I)$; not $\mathcal{O}(N|\mathcal{M}|)$, which would have been the case if Brute-force method was applied. Lastly, even though the complexity of P1 is $\mathcal{O}(N_I)$, it will not be computationally expensive as typically the value of N considered is in the range of 10 to 15 or even lesser, and always we have $N_I < N$. Hence given these values, it does not matter computationally even if the Brute-force method is employed.

The same logic applies to P2-P4 (discussed next) as well, where the search space is always the set of N_I idle or N_B busy channels, but not both simultaneously.

C. Secondary Energy Harvesting

Function $f_{H,t}$ (defined here) estimates the amount of harvested energy over a busy channel in t slots. $f_{H,t}$, like $f_{T,k}$, is also based on the current channel state X_0. The analysis corresponding to $f_{H,t}$ is relegated to Appendix B.

The scenario described above, *i.e.,* the choice of $\theta^{\text{Tx}}_{i,k}$ for data transmission, is when SU has sufficient energy to perform the data transmission, *i.e.,*

$$E(t) - E_{\text{req}}(j) \geq E_{\min}. \tag{11}$$

On the contrary it may happen that (11) does not hold, *i.e.,* $E(t)$ is not sufficient to carry out data transmission. In this situation, SU opts to harvest energy from channel $\theta^{\text{H}}_b \in \Theta_B$. θ^{H}_b is a particular θ_b which minimizes the objective in P2.

$$\text{(P2)} \quad : \underset{\theta_b}{\text{minimize}}\ \beta(\theta_b) \tag{12}$$

$$\begin{aligned} \text{subject to} \quad & C4 : f_{H,\beta}(\theta_b) \geq E_{\min} + E_{\text{req}}(j) - E(t), \\ & C5 : \beta \leq f_B(\theta_b), \\ & C6 : \beta \leq D_{\max}, \\ & C7 : \theta_b \in \Theta_B. \end{aligned}$$

(12) implies that SU chooses a particular $\theta^{\text{H}}_b \in \Theta_B$, which is presently occupied by a PU, estimated to be continuously occupied by the same PU for a duration of β slots, and from which the SU is able to successfully harvest in minimum time the extra amount of energy that it requires to perform the data transmission. Note that SU does not harvest energy from θ^{H}_b during the entire $f_B(\theta_b)$, but only for an interval β, which is sufficient to harvest the required energy for data transmission.

On the other hand, there may be a situation where SU has no data to transmit. In that case, SU enters sleep mode if $E(t) = E_{\max}$ and if $E(t) < E_{\max}$, then it chooses a $\theta^{\text{HN}}_b \in \Theta_B$ to enter the EH mode. θ^{HN}_b is a particular θ_b which minimizes the objective in P3:

$$\text{(P3)} \quad : \underset{\theta_b}{\text{minimize}}\ \sigma(\theta_b) \tag{13}$$

$$\begin{aligned} \text{subject to} \quad & C8 : f_{H,\sigma}(\theta_b) \geq E_{\max} - E(t), \\ & C9 : \sigma \leq f_B(\theta_b), \\ & C7 \text{ from } (12). \end{aligned}$$

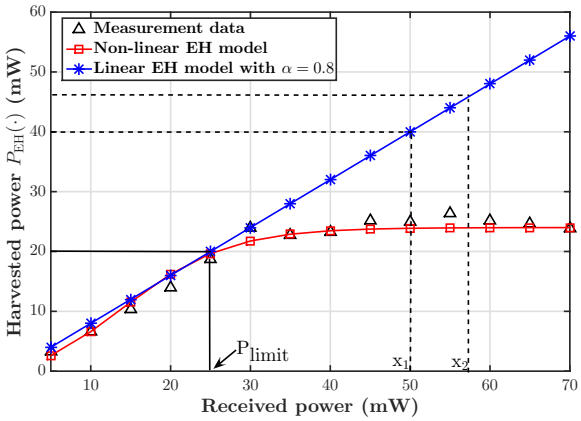

Fig. 3. A comparison among the measurement data from [36], the RF-DC power transfer functions for linear energy harvesting model with $\alpha = 0.8$, and the non-linear EH model [24].

At times, it may happen that data arrives for transmission when SU is in EH mode. In that case, the data has to suffer a delay until the harvesting process is complete and $E(t) = E_{\max}$. Hence in this case, the delay bound of the data gets modified as $D'_{\max} = D_{\max} - \sigma + t_{arr}$, where $1 \leq t_{arr} \leq \sigma$ is the slot in which the data arrives when SU is already in EH mode.

On the contrary when SU is fully charged, *i.e.,* $E(t) = E_{\max}$ but has no data to transmit, it enters sleep mode and performs duty cycling [35]. The aim of incorporating duty cycling in SU is to reduce energy wastage; it essentially means making a compromise between active and sleep mode.

In this context, we highlight the technical challenge introduced by the practical non-linear EH model and how our proposed protocol successfully handles it.

For a given P_p, let two busy PU-SU channel gains be $d_1^{-\alpha/2}h_1$ and $d_2^{-\alpha/2}h_2$. The corresponding received powers at the SU are $\text{x}_1 = P_p d^{-\alpha}|h_1|^2$ and $\text{x}_2 = P_p d^{-\alpha}|h_2|^2$, for which the estimated harvested power is $P_{\text{EH}}(\text{x}_1)$ and $P_{\text{EH}}(\text{x}_2)$, respectively. Fig. 3 demonstrates that the theoretical linear EH model suggests a one-to-one mapping of received power and harvested power at SU, *i.e.,* $P_{\text{EH}}(\text{x}_1) \neq P_{\text{EH}}(\text{x}_2)$ if $\text{x}_1 \neq \text{x}_2$. It also suggests $P_{\text{EH}}(\text{x}_1) > P_{\text{EH}}(\text{x}_2)$ if $\text{x}_1 > \text{x}_2$, and vice-versa. On the contrary, this is not the case as observed from the measurement data, which is also closely captured by the non-linear EH model considered in this work. From Fig. 3 it is clearly observed that, with the non-linear EH model we have $P_{\text{EH}}(\text{x}_1) \approx P_{\text{EH}}(\text{x}_2)$ even if $\text{x}_1 \neq \text{x}_2$. In other words, unlike the non-linear EH model, the linear EH model over-estimates the harvested power of practical EH circuits. This may at times lead to a wrong choice of θ^C_b if the decision is made solely based on the estimated harvested power.

In such scenarios, the proposed protocol chooses the 'busier' active PU channel, *i.e.,* the PU channel with a higher μ, for energy harvesting. Hence in this case, if we have $\mu_1 > \mu_2$, the busy PU channel corresponding to x_1 will be chosen by the SU over the one corresponding to x_2 in spite of having $\text{x}_1 < \text{x}_2$, which is counter-intuitive. This is because the expression (6) suggests that a higher μ will lead to a higher ζ_B.

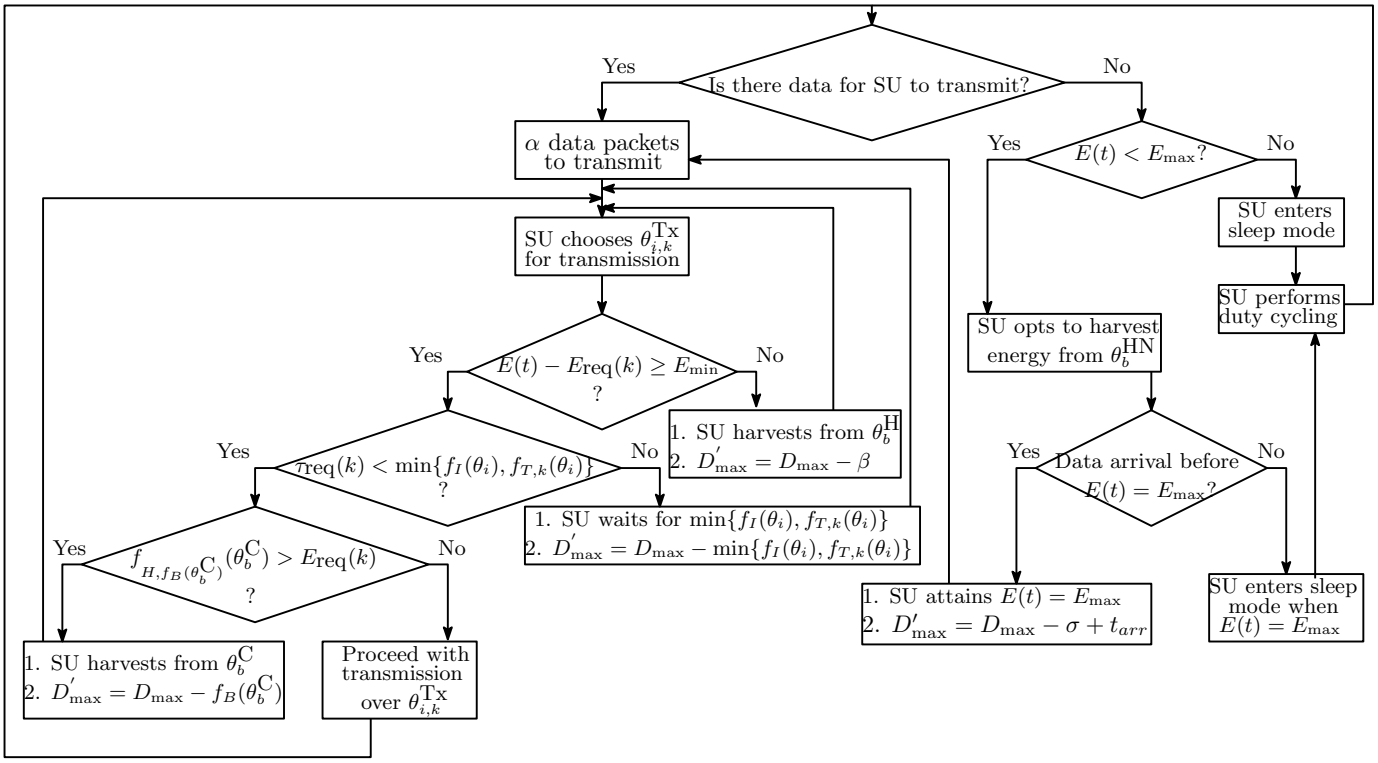

Fig. 4. Flow chart of the proposed protocol.

Hence we infer that, *when a SU has to choose a PU channel from a set of active PU channels for the purpose of energy harvesting, the decision should not be solely based on received power at the harvester or solely by the traffic characteristics of the PUs; instead these should be jointly considered such that the energy harvested over a certain time interval is maximized.*

D. Harvest or Transmit?

The proposed framework in its present form suggests energy harvesting in either of the following situations:

- SU has insufficient energy for data transmission.
- $E(t) < E_{\max}$ and there is no data for transmission.

Instead, now we introduce some 'intelligence' in the proposed framework in order to decide when to transmit or harvest. Till now, data transmission is suggested when (11) is satisfied, *i.e.,* $E(t) - E_{\mathrm{req}}(j) \geq E_{\min}$. But it may happen that, if energy harvesting is opted instead of data transmission, then the harvested energy will be greater than $E_{\mathrm{req}}(j)$, *i.e.,* there can be scenarios when harvesting could be a better option compared to transmission even with $E(t) - E_{\mathrm{req}}(j) \geq E_{\min}$. We introduce this intelligent selection of mode at the SU as discussed below:

With $E(t) - E_{\mathrm{req}}(j) \geq E_{\min}$, SU makes an intermediate choice of a busy channel $\theta_b^{\mathrm{C}} \in \Theta_B$ for energy harvesting, which maximizes the objective in P4:

$$\text{(P4)} \quad : \underset{\theta_b}{\text{maximize}} \; f_{H,f_B(\theta_b)}(\theta_b) \tag{14}$$

$$\text{subject to} \quad C10 : f_B(\theta_b) \leq D_{\max},$$

$$C7 \text{ from } (12).$$

If the estimated energy harvested over θ_b^{C} in $f_B(\theta_b^{\mathrm{C}})$ slots, *i.e.,* $f_{H,f_B(\theta_b^{\mathrm{C}})}(\theta_b^{\mathrm{C}})$ is more than $E_{\mathrm{req}}(j)$, SU chooses to delay the data transmission for $f_B(\theta_b^{\mathrm{C}})$ slots and it enters the EH mode provided $f_B(\theta_b^{\mathrm{C}}) \leq D_{\max}$. Note that now the delay bound for the data becomes $D'_{\max} = D_{\max} - f_B(\theta_b^{\mathrm{C}})$. This 'time-varying' monotonically decreasing delay bound guarantees the timely delivery of data packets. In other words, when $E(t) - E_{\mathrm{req}}(j) \geq E_{\min}$,

$$\text{SU Action} = \begin{cases} \text{Harvest over } \theta_b^{\mathrm{C}} & f_{H,f_B(\theta_b^{\mathrm{C}})}(\theta_b^{\mathrm{C}}) > E_{\mathrm{req}}(j) \\ \text{Transmit over } \theta_{i,k}^{\mathrm{Tx}} & \text{else.} \end{cases} \tag{15}$$

Remark 1. *Note that unlike the existing works, choice of θ_b^C is based on both the current channel state and the traffic characteristics of PU.*

We define this entire procedure as our proposed protocol, which is presented in the form of a flowchart in Fig. 4.

E. Description of Performance Measures

Here we analytically characterize the performance of the proposed protocol in terms of data rate, energy consumption, and energy efficiency[2] as defined below.

Without any loss of generality, the sensing duration and the feedback packets are assumed to be very small compared to slot duration, *i.e.,* $T_{pr} = \Upsilon T_s$ $(\Upsilon \ll 1)$ [37].

[2]The performance metrics defined here are all with respect to the SU. Thus the term 'SU' is not explicitly mentioned in each of them.

Definition 2. *Data rate D_R is defined as long-term average of the successful SU transmissions per second.*

$$D_{\mathrm{R}} = \lim_{X\to\infty} \frac{1}{X} \sum_{a=1}^{X} \frac{\Lambda \gamma_{\mathrm{opt}}(a) R_i(a)}{\gamma_{\mathrm{opt}}(a) T_s + 2T_{pr}}. \tag{16}$$

Here $\Lambda = (1-\epsilon_0)(1-\delta)(1-P_b)(1-\kappa)$, R_i is the rate of chosen modulation, i and $2T_{pr}$ account for the two-way handshake between Rx and Tx.

Definition 3. *Effective energy consumption E_{EC} is defined as the long-term average energy consumption by SU per unit successful data delivery.*

By this definition,

$$E_{\mathrm{EC}} = \lim_{X\to\infty} \frac{1}{X} \sum_{p=1}^{X} \frac{e_{\mathrm{C}}(p) - e_{\mathrm{H}}(p)}{\Lambda \gamma_{\mathrm{opt}}(p) R_i(p)}. \tag{17}$$

Here $e_{\mathrm{C}}(p)$ and $e_{\mathrm{H}}(p)$, respectively denote the energy consumption due to data transmission and energy harvested as:

1) $e_{\mathrm{C}}(p) = \gamma_{\mathrm{opt}}(p)\varepsilon_t + \gamma_{\mathrm{opt}}(p)\varepsilon_{\mathrm{idle}} + 2\varepsilon_p + \varepsilon_s$, where $\varepsilon_t = P_t T_s, \varepsilon_{\mathrm{idle}} = P_{\mathrm{idle}} T_s, \varepsilon_p = P_{\mathrm{prob}} T_s$, and $\varepsilon_s = P_{\mathrm{sense}} T_s$ denote per-slot transmission, idling, probing, and sensing energy, respectively.
2) $e_{\mathrm{H}}(p)$ consists of: (a) energy harvested when there is insufficient energy at SU for data transmission, (b) energy harvested when there is no data to transmit and $E(t) < E_{\max}$, and (c) energy harvested 'intelligently' even when there is data to be transmitted.
Accordingly we obtain:

$$e_{\mathrm{H}}(p) = \mathbb{1}_{\{\theta_b^{\mathrm{H}}\}} \cdot \underbrace{f_{H,\beta(p)}(\theta_b^{\mathrm{H}})}_{\substack{\text{(a)}\\ \text{From (12)}}} + \mathbb{1}_{\{\theta_b^{\mathrm{HN}}\}} \cdot \underbrace{f_{H,\sigma(p)}(\theta_b^{\mathrm{HN}})}_{\substack{\text{(b)}\\ \text{From (13)}}} + \mathbb{1}_{\{\theta_b^{\mathrm{C}}\}} \cdot \underbrace{f_{H,f_B(\theta_b^{\mathrm{C}})(p)}(\theta_b^{\mathrm{C}})}_{\substack{\text{(b)}\\ \text{From (14)}}} \tag{18}$$

where $\mathbb{1}_{\{x\}}$ is an indicator function that takes 1 when x holds and 0 otherwise. $\mathbb{1}_{\{\theta_b^{\mathrm{H}}\}}$, $\mathbb{1}_{\{\theta_b^{\mathrm{HN}}\}}$, and $\mathbb{1}_{\{\theta_b^{\mathrm{C}}\}}$ mathematically guarantee that only one of (a), (b), and (c) occurs at any particular point of time.

Remark 2. *Note that, both β and $f_B(\theta_b^C)$ are functions of PU arrival statistics. On the other hand, summand $P_{EH}(X_0)$ is a function of present channel state. Thus, $e_H(p)$ can be said to be a joint function of PU arrival statistics as well as present channel state, which is a major contribution of this work.*

Given that it is intuitive to have higher data rate D_R for a higher effective energy consumption E_{EC}, the trade-off between the two is efficiently captured by the performance metric 'energy efficiency' η. η is defined as [38]:

$$\eta = \frac{D_R}{E_{\mathrm{EC}}}. \tag{19}$$

It is to be noted that as both D_R and E_{EC} are functions of both ϵ_0 and δ, η is also the same.

TABLE III
TRANSMISSION MODES.

X_T (dBm)	Modulation	R_n (bits/sym.)
$X_0 < 6.9897$	No transmission	0
$6.9897 \le X_0 < 10.0000$	BPSK	1
$10.0000 \le X_0 < 11.7609$	QPSK	2
$11.7609 \le X_0 < 13.0103$	8-QAM	3
$13.0103 \le X_0 < 13.9794$	16-QAM	4
$13.9794 \le X_0 < 14.7712$	32-QAM	5
$14.7712 \le X_0$	64-QAM	6

IV. NUMERICAL RESULTS

Here we evaluate the performance of the proposed protocol via extensive simulations and compare its performance with nearest existing approaches.

From (8) we know $P_b = 2\exp\left(\frac{-1.5X^2(z)}{N_0 B(j-1)}\right)$ for M-QAM constellations [34]. The thresholds $X_{T_k}\ \forall\ k = 0, \cdots, |\mathcal{M}-2|$ are determined based on the acceptable P_b of the application at hand. Noise power is set to unity without any loss of generality, *i.e.,* $N_0 B = 1$ [39]. Using $P_b = 10^{-3}$ [34], $P_t = 40$ mW, and values of all the constants, we obtain the transmission modes of $X = \sqrt{P_t d^{-\alpha}}|h|$ as in Table III.

We consider 10 PUs with each of them acquiring a primary channel, and randomly select their respective μ_n and λ_n. Distance of all PUs from the SU is randomly chosen from the set $[2, 3]$ m. Moreover, the SU Tx-Rx distance is 3 m and the corresponding path loss factor $\alpha = 3$ [40].

Data transmission over a Rayleigh channel is considered here, though the proposed framework is equally valid for all fading scenarios. The default parameters considered as: carrier frequency $f_c = 900$ MHz, slot duration $T_s = 100$ μs [41], and $\Upsilon = 0.2$ [37]. Propagation delay is ignored considering the short-range communication scenario. Here the average PU activity duty cycle is $\psi = \frac{\mathbb{E}[ON]}{\mathbb{E}[ON]+\mathbb{E}[OFF]}$. PU transmission power $P_p = 500$ mW and with respect to SU, sensing/probing, idling, and transmission consumptions are 40 mW, 16.9 mW, and 69.5 mW, respectively [42].

For the battery at SU, a regular 1.2 V/1.15 Ah NiMH battery is considered. We have $E_{\max} = 1.2$ V $\times$ 1.15 A $\times$ 3600 s $= 4.968$ kJ [43] and we assume $E_{\min} = 0.05 \cdot E_{\max}$. Moreover, we assume $D_{\max} = 50$ ms [44]. Lastly from (3) we know that $P_{\mathrm{EH}} = \frac{M(1 - e^{-aP_p d^{-\alpha}|h_{ps}|^2})}{1 + e^{-a(P_p d^{-\alpha}|h_{ps}|^2 - b)}}$, where M, a, and b are circuit parameters. In this work, we have considered $M = 24$ mW, $a = 150$, and $b = 0.014$ [36].

A. Verification of ζ_B, ζ_I, and $\zeta_{k,k+1}$ Through Simulation

1) ζ_B: The average 'OFF' duration is taken as 5 ms and the analytically obtained ζ_B using (6) is compared with Monte Carlo simulations. As observed in Fig. 5, ζ_B increases monotonically with ψ. However, the rate of increase shoots up as $\psi \longrightarrow 1$. This is intuitive also; the 'degree of busyness' of the channel increases with increasing ψ. It is also to be noted that for any particular ψ, $\delta_1 > \delta_2$ implies that ζ_B for δ_1 is

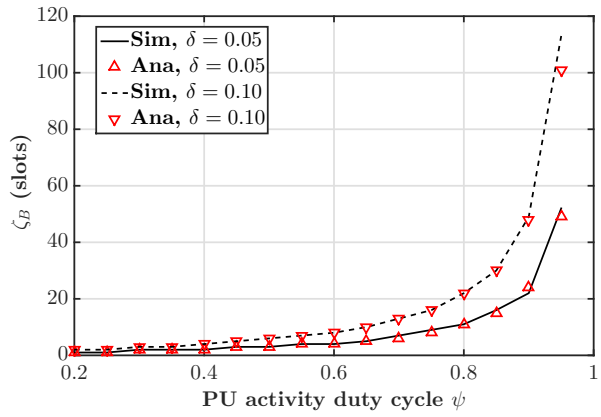

Fig. 5. Verification of ζ_B estimation via Monte Carlo simulation.

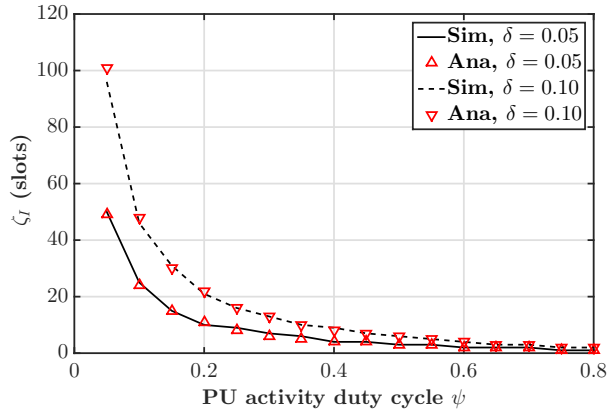

Fig. 6. Verification of ζ_I estimation via Monte Carlo simulation.

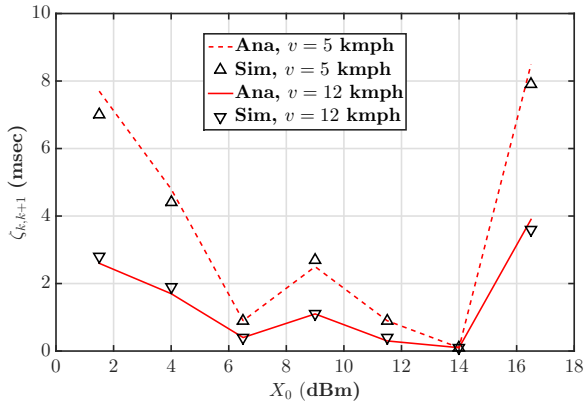

Fig. 7. Verification of $\zeta_{k,k+1}$ estimation. $\epsilon_0 = 0.05, \kappa = 0$.

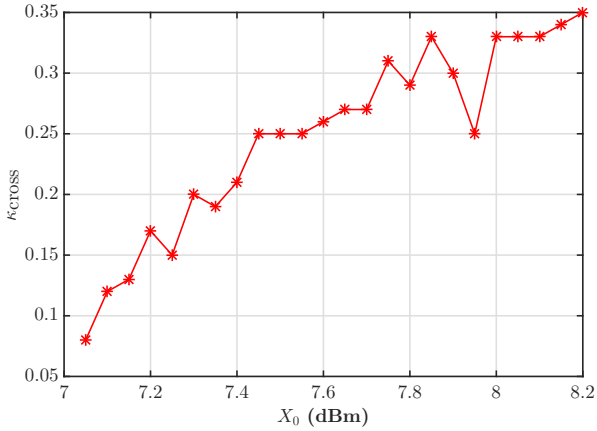

Fig. 8. Effect of κ on X_0.

more than ζ_B for δ_2 and the gap between the two increases monotonically as $\psi \longrightarrow 1$.

2) ζ_I: Here the average 'ON' duration is taken as 5 ms to compare the analytical ζ_I with the one obtained by Monte Carlo simulations. As observed in Fig. 6, ζ_I decreases with ψ unlike ζ_B. This is also intuitive; the 'degree of idleness' of the channel decreases with increasing ψ. Lastly, for any particular ψ, $\delta_1 > \delta_2$ implies that ζ_I for δ_1 is more than ζ_I for δ_2 and the gap between the two decreases monotonically as $\psi \longrightarrow 1$.

Hence, ζ_B and ζ_I can be said to be 'dual' of each other.

3) $\zeta_{k,k+1}$: Fig. 7 demonstrates that the analytically obtained $\zeta_{k,k+1}$ matches closely with the exhaustive Monte Carlo simulations. As expected, current channel state X_0 plays a critical role in determining $\zeta_{k,k+1}$ for a given set of system parameters. X_0 close to any of the thresholds has relatively lesser $\zeta_{k,k+1}$ compared to those X_0 that are away from the thresholds. Lastly, it is also to be observed, that slower the channel variation, higher is the $\zeta_{k,k+1}$ for any particular X_0.

B. Effect of CSI imperfection on X_0

As stated in Section II-D, Tx receives imperfect X_0 in real-world communication scenarios. To account for this, in this section we demonstrate the effect of CSI imperfection parameter κ on current channel state X_0.

Note that, if $X_0 \in [X_{T_k}, X_{T_{k+1}})$ but $\widehat{X}_0 \notin [X_{T_k}, X_{T_{k+1}})$, then it will lead to an incorrect choice of modulation. From (4) we know that, the higher the value of κ, the higher is the deviation of X_0 from its true value. In Fig. 8 we demonstrate the effect of κ on a range of values of X_0. In this figure, we plot the minimum κ (κ_{cross}) that results in a $\widehat{X}_0 \notin [X_{T_k}, X_{T_{k+1}})$ when $X_0 \in [X_{T_k}, X_{T_{k+1}})$.

Fig. 8 considers X_0 in the range of $[7, 8.2]$ dBm. From Table III we know that this entire range falls in the BPSK domain, *i.e.,* $[6.9897, 10.000)$ dBm. We observe that, as we move deeper into the region, *i.e.,* as we move towards 8.2 dBm from 7 dBm in this case, the value of κ_{cross} also follows an upward trend. This is intuitive also; relatively lesser CSI imperfection is enough to result in $\widehat{X}_0 \notin [X_{T_k}, X_{T_{k+1}})$ when $X_0 \in [X_{T_k}, X_{T_{k+1}})$ for the values of X_0 lying nearer to a threshold. It can also be noted that, the lack of smoothness in the plot is attributed to the random nature of the error term e in (4), *i.e.,* $\mathrm{e} \sim \mathcal{CN}(0, 1)$.

C. Effect of Channel Variation on Data Rate

In this section the effect of current channel state X_0 on data rate D_R is demonstrated. In the proposed protocol, SU uses a probing signal and its respective feedback once in $\zeta_{k,k+1}$ unlike conventional AMC [45], which uses a probing signal in

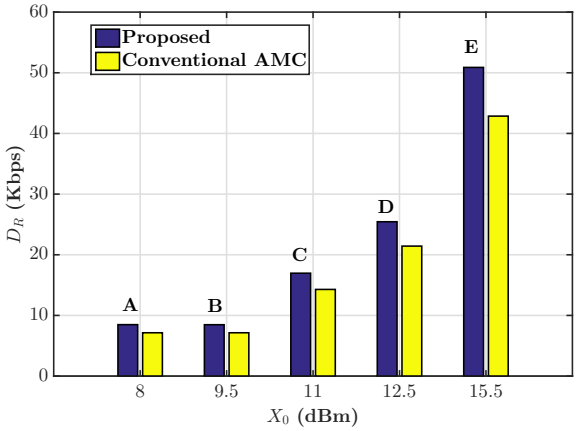

Fig. 9. Effect of X_0 on data rate D_R. $\kappa = 0$, $v = 2$ kmph, $\epsilon_0 = 0.10$, $\mu = 5$ ms, $\psi = 0.05$, and $\delta = 0.05$.

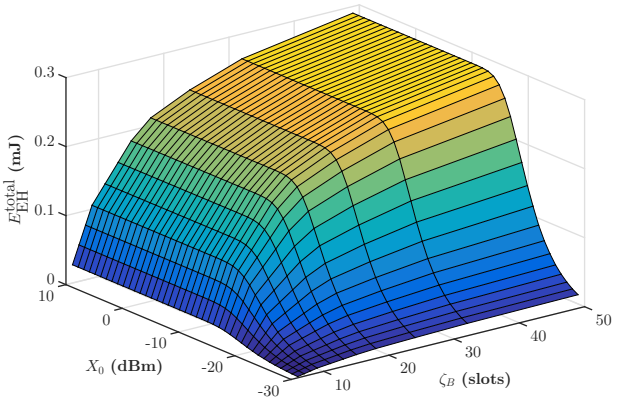

Fig. 10. Effect of ζ_B and X_0 on $E_{\text{EH}}^{\text{total}}$. $\kappa = 0$, $v = 5$ kmph, $\lambda = 5$ ms, $\delta = 0.05$, and $\rho_{\min} = 0.9$.

TABLE IV
OVERHEAD REDUCTION.

X_0 (dBm)	8	9.5	11	12.5	15.5
Overhead reduction (%)	97.9592	97.6190	97.9592	97.9592	97.9592

each slot to adjust the modulation scheme. Thus we compare the data rate of both, where data rate as defined in Section III-E is the number of successful transmissions per second.

As observed from Fig. 9, D_R corresponding to case E is the highest; this is because according to Table III, case A, B, C, D and E correspond to the modulation scheme BPSK, BPSK, QPSK, 8-QAM, and 64-QAM, respectively. Irrespective of X_0, a gain of around 18% in D_R is also observed in the figure with respect to conventional AMC. This gain is due to the reduced overhead in the proposed protocol.

Lastly, Table IV demonstrates that though the gain in terms of D_R is around 18%, it results in overhead reduction of about 97.96% irrespective of X_0.

D. Effect of PU Traffic Characteristics and Channel State on Harvested Energy

Here we demonstrate the importance of both the present channel state X_0 and PU traffic characteristics on the total harvested energy $E_{\text{EH}}^{\text{total}}$, as observed in Fig. 10. A scenario is considered when the SU needs to harvest from the set of channels over which PUs are currently present.

From (6) we know that for same δ, higher μ results in higher ζ_B and hence higher are the chances of energy harvesting. This is also observed in Fig. 10 where for $\lambda = 5$ ms and $X_0 = -16$ dBm, $\zeta_B = 6$ slots when $\psi = 0.7$ compared to $\zeta_B = 49$ slots when $\psi = 0.95$.

It is interesting to observe from the figure that, it is not enough to choose that channel which has the PU with highest μ. The channel in between the chosen PU and the SU is also a critical factor. If the channel with highest μ PU is selected with the channel between the corresponding PU and SU is in deep fade, it is not of any use; with $\zeta_B = 49$ slots (*i.e.,* $\psi = 0.95$), $E_{\text{EH}}^{\text{total}} = 0.0197$ mJ when $X_0 = -30$ dBm compared to $E_{\text{EH}}^{\text{total}} = 0.2904$ mJ when $X_0 = 10$ dBm. This implies that if the additional 'PU-SU channel' factor is also accounted in the EH process, it results in as high as 13.74 times gain in the harvested energy.

As discussed in Section III-C, we further observe here that scenarios may arise, where a smaller X_0 may lead to a higher $E_{\text{EH}}^{\text{total}}$; $X_0 = -18$ dBm results in $E_{\text{EH}}^{\text{total}} = 0.2151$ mJ for $\zeta_B = 32$ slots against $X_0 = -5$ dBm, which results in $E_{\text{EH}}^{\text{total}} = 0.1584$ mJ for $\zeta_B = 13$ slots. Hence we reaffirm our claim that the channel for harvesting should be decided jointly by X_0 and μ, not individually.

Lastly, a 'flat' region is also to be observed in the figure, where $E_{\text{EH}}^{\text{total}}$ does not change irrespective of change in X_0. For instance with $\zeta_B = 49$ slots, $E_{\text{EH}}^{\text{total}} = 0.2904$ mJ for both $X_0 = 8, 10$ dBm. This region corresponds to Proposition 1 in Appendix B, *i.e.,* $X_{0,1} \neq X_{0,2}$ does not essentially guarantee $E_{\text{EH}}^{\text{total}}(X_{0,1}) \neq E_{\text{EH}}^{\text{total}}(X_{0,2})$.

E. Effect of PU Traffic Characteristics on Data Rate

Here we investigate the effect of traffic characteristics of the idle PU channel that is chosen by the SU for data transmission. Fig. 11 demonstrates a non-increasing trend of data rate D_R against PU activity duty cycle ψ. This is intuitive also; as from (7) we know that ζ_I is directly proportional to λ for a given δ. It is interesting to note that the variation in v does not show any change in D_R after a certain point, which appears to be counter-intuitive when compared against Fig. 7. The explanation behind this observation is already stated in Section III-B, i.e, $\tau_{\text{req}}(k) \leq \min\{f_I(\theta_i), f_{T,k}(\theta_i)\}$. This justifies Fig. 11 based on the fact that neither of $f_I(\theta_i)$ or $f_{T,k}(\theta_i)$ but their combined effect defines the data rate D_R. Lastly, this figure also justifies that selection of empty channel solely based on channel state is not a wise decision; the traffic characteristics should also be taken into account.

F. Effect of PU Traffic Characteristics and Channel State on Energy Efficiency

Based on the observations made above, now we investigate the combined effect of (a) the traffic characteristics of active

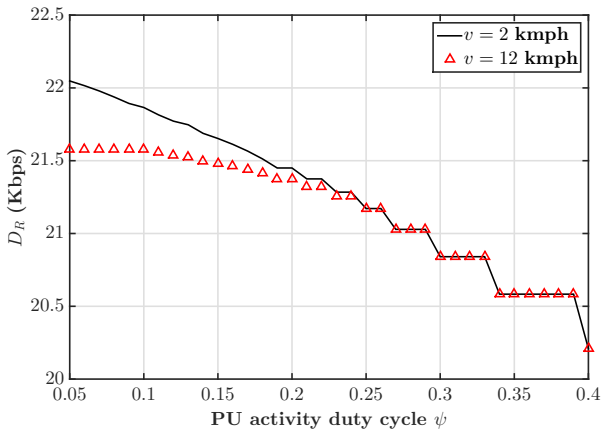

Fig. 11. Effect of PU duty cycle ψ on D_R. $\kappa = 0$, $\mu = 5$ ms, $\delta = 0.05$, and $\epsilon_0 = 0.10$.

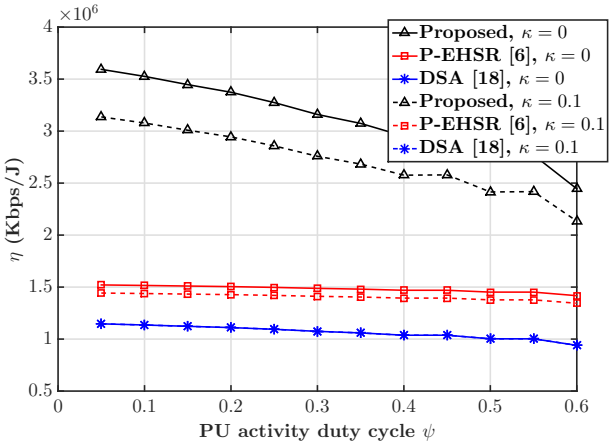

Fig. 13. Performance comparison. $\mu = 5$ ms, $\epsilon_0 = 0.10, \delta = 0.05$, and $\rho_{\min} = 0.9$.

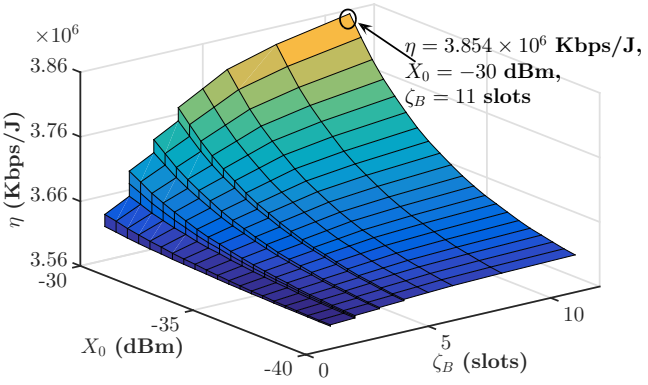

Fig. 12. Effect of ζ_B and X_0 on η. $\kappa = 0$, $v = 2$ kmph, $\epsilon_0 = 0.10$, $\lambda = 5$ ms, $\delta = 0.05$, and $\rho_{\min} = 0.9$.

PUs and (b) the channel between each active PU and the SU, on the system energy efficiency η. From (16), (17), and (19) it is noted that $\eta_{\max}$ is attained where the energy harvested is maximum, *i.e.,* when the active PU with the highest μ and the best PU-SU channel is chosen. This is also observed in Fig. 12; $\eta_{\max} = 3.854 \times 10^6$ Kbps/J when $X_0 = -30$ dBm and $\zeta_B = 11$ slots.

Thus Fig. 12 in a way reinstates the point that was made in Section III-C and Fig. 10 regarding the fact that maximum energy is harvested only across the active PU with both the highest μ and the best X_0, such that both the energy harvested within a time interval and hence the system η is maximized.

G. Performance Comparison

In this section we compare the performance of the proposed protocol with the existing benchmark schemes, which are:

1) DSA [6]: SU in this scheme upon entering a PU channel, decides to transmit if it is found idle. It estimates the time for which the channel will continue to remain idle and transmits consecutively for those number of slots. This scheme does not involve any EH mode.
2) P-EHCR [18]: SU in this scheme predicts the PU activity and accordingly decides whether to transmit or harvest from the channel accordingly. Moreover it also employs a linear EH model with a fixed energy conversion efficiency α, *i.e.,* Harvested power $= \alpha \cdot$ Received power.

Fig. 13 demonstrates the comparison with the existing approaches in terms of energy efficiency η against PU activity duty cycle ψ, which demonstrates an overall decreasing trend. This trend was also earlier observed in Fig. 11, where data rate D_R was varied against ψ.

It is observed from the figure that DSA performs the poorest among the three schemes, because it decides the duration of data transmission solely based on the PU traffic characteristics; it does not consider the channel state or perform energy harvesting. P-EHCR performs better compared to DSA because not only it performs PU activity prediction, but it also harvests energy. The proposed protocol performs the best; obtaining η as high as about 1.36 times of the nearest existing approach. This enhanced performance is attributed to the inherent 'intelligence' of the proposed protocol, that not only decides when to harvest/transmit but also over which active/idle PU channel and for how long. Moreover, the proposed protocol, unlike DSA and P-EHCR, also involves channel dependent modulation scheme variation.

Lastly, we also note that the performance degradation occurs with $\kappa \neq 0$ in the proposed protocol as well as in P-EHCR. This is intuitive; it depends on the application that dictates the acceptable limit of κ. However, DSA does not show any performance degradation with $\kappa \neq 0$, because it does not depend on the channel state but operates purely based on the PU traffic characteristics.

V. Conclusion

In this paper we have proposed a new energy-aware link-layer protocol for the SUs in EH-CRNs. The proposed protocol optimally decides when and over which channel to transmit or harvest. It also decides the transmission or harvesting duration over a chosen channel, that accounts for the SU delay budget. Through rigorous analysis we have demonstrated that, while

choosing a channel for transmission or harvesting, in addition to PU traffic characteristics, the channel states between SU-Tx−SU-Rx and PU−SU-Tx along with SU delay and energy state play very important roles. Extensive simulations have validated the proposed analysis. Numerical results have showcased the significance of the proposed protocol in terms of much enhanced energy efficiency.

APPENDIX A
$f_{T,k}$ ESTIMATION

Let present channel state $X(t) = X_0$ and we assume $X_0 \in [X_{T_k}, X_{T_{k+1}})$. Note that the probability density function of $X(t)$, *i.e.,* $f_X(x)$ depends on the underlying fading model. However, the time derivative of $X(t)$, *i.e.,* $\dot{X}(t) \triangleq \frac{dX(t)}{dt}$ is a zero mean Gaussian random variable (RV) irrespective of the fading distribution, *i.e.,* $\dot{X}(t) \sim \mathcal{N}(0, \dot{\sigma})$, when d and α are constant [46].

Based on this unique property of $\dot{X}$ (index t is removed for brevity), a framework was developed in [8], [47] to dynamically estimate both the optimal 'sleep' duration and 'transmission' duration. This framework is used here to define function $f_{T,k}$ that estimates the time $\zeta_{k,k+1}$, during which X will continue to be $[X_{T_k}, X_{T_{k+1}})$ when $X_0 \in [X_{T_k}, X_{T_{k+1}})$. It should be noted here that the SU transmits data with modulation m_{k+1} during this estimated duration $\zeta_{k,k+1}$.

Based on X_0, we obtain X in the next time slot as:

$$X(t+T_s) = X(t) + \dot{X}\cdot T_s + \ddot{X}\cdot\frac{T_s^2}{2} + \cdots \approx X_0 + \dot{X}\cdot T_s \quad (\because T_s \ll 1). \tag{A-2}$$

Thus, probability that $X(t+T_s) \in [X_{T_k}, X_{T_{k+1}})$ is

$$\Pr\left\{X_{T_k} \le X(t+T_s) < X_{T_{k+1}}\right\} \overset{\text{by } (A-2)}{\approx} \Pr\left\{X_{T_k} \le X_0 + X_1 < X_{T_{k+1}}\right\}. \tag{A-3}$$

Here $X_1 (= \dot{X}\cdot T_s)$ represents the temporal variation of X in the next slot. Thus, $X_1 \sim \mathcal{N}(0, \dot{\sigma}_1)$ where $\dot{\sigma}_1 = T_s\dot{\sigma}$. X_1 being Gaussian in nature implies that $X_1 \in (-\infty, +\infty)$. Note that X is signal envelope, *i.e.,* a non-negative quantity and hence, $X_1 \in [-X_0, \infty)$. In other words, X_1 does not follow a Gaussian, but truncated Gaussian distribution:

$$f_{X_1}(\beta) = \begin{cases} \frac{1}{1-\Phi_1\left(-\frac{X_0}{\dot{\sigma}_1}\right)} \frac{1}{\sqrt{2\pi}\dot{\sigma}_1} e^{\left(\frac{-\beta^2}{2\dot{\sigma}_1{}^2}\right)} & -X_0 \le \beta \\ 0 & \text{elsewhere.} \end{cases} \tag{A-4}$$

Here $\Phi_1(x) = \int_{-\infty}^{x} \frac{1}{\sqrt{2\pi}} e^{-\frac{t^2}{2}} dt$ is the cumulative distribution function of standard univariate normal distribution and $\dot{\sigma}_1$ depends on the underlying fading model. Accordingly we obtain (A-3) as $\Pr\left\{X_{T_k} \le X_0 + X_1 < X_{T_{k+1}}\right\} = \int_{X_{T_k}-X_0}^{X_{T_{k+1}}-X_0} f_{X_1}(\beta)d\beta$. Similarly, the probability that X will continue to stay in $[X_{T_k}, X_{T_{k+1}})$ in next γ slots is

$$\Pr\left\{X_{T_k} \le X_0 + X_1 < X_{T_{k+1}}, \cdots, X_{T_k} \le X_0 + X_\gamma < X_{T_{k+1}}\right\}, \tag{A-5}$$

where X_γ is a zero mean truncated Gaussian RV with variance $\dot{\sigma}_\gamma^2 = \gamma\dot{\sigma}_1^2$. As $X_1, X_2, \cdots, X_\gamma$ are in general not independent,

$$\Pr\left\{X_{T_k} \le X_0 + X_1 < X_{T_{k+1}}, \cdots, X_{T_k} \le X_0 + X_\gamma < X_{T_{k+1}}\right\} = \int_{X_{T_k}-X_0}^{X_{T_{k+1}}-X_0} \cdots \int_{X_{T_k}-X_0}^{X_{T_{k+1}}-X_0} f_{\underline{X_\gamma}}(\underline{x_\gamma}, \Sigma, \underline{X_{\gamma 0}}) d\underline{x_\gamma}, \tag{A-6}$$

where $f_{\underline{X_\gamma}}(\underline{x_\gamma}, \Sigma, \underline{X_{\gamma 0}})d\underline{x_\gamma}$ is the γ-variate truncated Gaussian distribution [48].

As we are interested in finding the optimum value of γ (say, γ_{opt}) for a given $X_0 \in [X_{T_k}, X_{T_{k+1}})$, we solve the optimization problem P1 in (A-1). Obtaining γ_{opt} ($\zeta_{k,k+1} = \gamma_{\text{opt}} \cdot T_s$) from P1 requires sequential search method, with γ starting from 1.

Function $f_{T,k}$ is actually the solution of P1 for a given set of system parameters (f_D, T_s, and ϵ_0) and a given X_0. Index T and k of $f_{T,k}$ denote the estimated time, and the chosen constellation, respectively.

APPENDIX B
$f_{H,t}$ ESTIMATION

From (3) we know that $P_{\text{EH}} = \frac{M(1 - e^{-aP_p d^{-\alpha}|h_{ps}|^2})}{1 + e^{-a(P_p d^{-\alpha}|h_{ps}|^2 - b)}}$, *i.e.,* P_{EH} is a function of the channel gain h_{ps} when all other parameters are constant. Note that M, a, and b are system parameters and P_p in this work also does not vary. Hence $P_{\text{EH}} = f(X_0)$ as $X_0 = \sqrt{P_p d^{-\alpha}}|h_{ps}(t)|$.

From (A-2) we also know that when $X(t) = X_0$, $X(t+T_s)$ can be approximated as $X(t+T_s) \approx X_0 + X_1$ with X_1 being a truncated Gaussian RV as expressed in (A-4). Similarly from (A-5) we obtain $X(t+\gamma.T_s) \approx X_0 + X_\gamma$ where X_γ is also a zero mean truncated Gaussian RV. However, this relation does not hold for any arbitrary value of γ but is dependent on the Clarke-Jakes correlation function $\rho(n) = J_0(2\pi f_D n T_s)$, where $J_0(\cdot)$ is Bessel function of first kind and of zeroth order, f_D is the maximum Doppler frequency, and nT_s is the temporal gap between the samples under consideration [30].

Upper limit of γ: Due to the oscillatory nature of $J_0(\cdot)$, $\rho(n)$ is not a monotonically decreasing function of n. Without any loss of generality, we consider the slow fading scenario in this work, *i.e.,* the $f_D n T_s < 0.2$ region [30]. This results in $\rho \in [1, 0.64]$. In this region of interest, a suitable polynomial expansion of $J_0(\cdot)$ is [49]:

$$J_0(x) \approx 1 - \frac{x^2}{4} + \frac{x^4}{64}. \tag{B-1}$$

Thus solving (B-1) for a particular acceptable $\rho_{\min} \in [1, 0.64]$, *i.e.,* by putting $1 - \frac{x^2}{4} + \frac{x^4}{64} = \rho_{\min}$, we obtain $\gamma_{\max}$ with respect to this particular $\rho_{\min}$. Note that $\gamma_{\max}$ is the maximum acceptable value of γ, for which we can state $X(t+\gamma.T_s) \approx X_0 + X_\gamma$ for a given $\rho_{\min}$. In other words, for a given $\rho_{\min}$

$$(\text{P5}) \quad : \underset{\gamma}{\text{maximize}}\ \gamma \tag{A-1}$$

$$\text{subject to} \quad C11: \quad \Pr\left\{X_{T_k} \leq X_0 + X_1 < X_{T_{k+1}}, \cdots, X_{T_k} \leq X_0 + X_\gamma < X_{T_{k+1}}\right\} \geq 1 - \epsilon_0,$$
$$C12: \quad \gamma \geq 0.$$

Here ϵ_0 is the 'acceptable error limit' of $X \notin [X_{T_k}, X_{T_{k+1}})$ and is a given system parameter.

$$X(t + \gamma.T_s) \approx X_0 + X_\gamma \quad \text{when} \quad 1 \leq \gamma \leq \gamma_{\max} \tag{B-2}$$

The above representation is useful in the context of (12), (13), and (14), where we need to estimate the amount of total harvested energy $E_{\text{EH}}^{\text{total}}$ based on X. When $X = X_0$,

$$E_{\text{EH}}^{\text{total}}(\gamma) = \sum_{i=1}^{\gamma} P_{\text{EH}}(i) \cdot T_s \tag{B-3}$$

where

$$P_{\text{EH}}(i) = \frac{M(1 - e^{-a(X_0 + X_i)^2})}{1 + e^{-a((X_0+X_i)^2 - b)}} \quad \forall \quad 1 \leq \gamma \leq \gamma_{\max}.$$

Hence $f_{H,t}$ maps a particular busy channel θ_b to $E_{\text{EH}}^{\text{total}}$, which is a joint function of X_0 and γ.

Proposition 1. *If* $X_{0,1} = \sqrt{P_p d_1^{-\alpha}}|h_1|$ *and* $X_{0,2} = \sqrt{P_p d_2^{-\alpha}}|h_2|$, *then for a given set of parameters, i.e.,* M, a, b, P_p, α *and* γ, $X_{0,1} \neq X_{0,2}$ *does not essentially guarantee* $E_{EH}^{total}(X_{0,1}) \neq E_{EH}^{total}(X_{0,2})$.

Proof. Given that $P_{\text{EH}}(i)$ is a non-decreasing function of the channel state X_0, it is intuitive that $X_{0,1} \geq X_{0,2}$ translates to $E_{\text{EH}}^{\text{total}}(X_{0,1}) \geq E_{\text{EH}}^{\text{total}}(X_{0,2})$. Note that the equality holds only when both $X_{0,i} \gg 1\ \forall\ i = 1, 2$, as in that case we have $P_{\text{EH}}(X_{0,i}) \approx M\ \forall\ i = 1, 2$. This results in having $E_{\text{EH}}^{\text{total}}(X_{0,1}) = E_{\text{EH}}^{\text{total}}(X_{0,2})$, even when $X_{0,1} \neq X_{0,2}$ for a given set of M, a, b, P_p, α and γ. □

REFERENCES

[1] "On the pulse of the networked society," Ericsson Mobility Report, Jun. 2017.

[2] M. Lopez-Benitez and F. Casadevall, "Time-dimension models of spectrum usage for the analysis, design, and simulation of cognitive radio networks," *IEEE Trans. Veh. Technol.*, vol. 62, no. 5, pp. 2091–2104, June 2013.

[3] W. Webb, "On using white space spectrum," *IEEE Commun. Mag.*, vol. 50, no. 8, pp. 145–151, Aug. 2012.

[4] S. Geirhofer, L. Tong, and B. M. Sadler, "COGNITIVE RADIOS FOR DYNAMIC SPECTRUM ACCESS - dynamic spectrum access in the time domain: Modeling and exploiting white space," *IEEE Commun. Mag.*, vol. 45, no. 5, pp. 66–72, May 2007.

[5] A. Mariani, S. Kandeepan, and A. Giorgetti, "Periodic spectrum sensing with non-continuous primary user transmissions," *IEEE Trans. Wireless Commun.*, vol. 14, no. 3, pp. 1636–1649, Mar. 2015.

[6] S. Agarwal and S. De, "Impact of channel switching in energy constrained cognitive radio networks," *IEEE Commun. Lett.*, vol. 19, no. 6, pp. 977–980, June 2015.

[7] H. Moon, "Channel-adaptive random access with discontinuous channel measurements," *IEEE J. Sel. Areas Commun.*, vol. 34, no. 5, pp. 1704–1712, May 2016.

[8] P. Mukherjee and S. De, "cDIP: Channel-aware dynamic window protocol for energy-efficient IoT communications," *IEEE Internet Things J.*, vol. 5, no. 6, pp. 4474–4485, Dec 2018.

[9] Q. Liu, S. Zhou, and G. B. Giannakis, "Cross-layer combining of adaptive modulation and coding with truncated ARQ over wireless links," *IEEE Trans. Wireless Commun.*, vol. 3, no. 5, pp. 1746–1755, Sep. 2004.

[10] X. Wang, Q. Liu, and G. B. Giannakis, "Analyzing and optimizing adaptive modulation coding jointly with ARQ for QoS-guaranteed traffic," *IEEE Trans. Veh. Technol.*, vol. 56, no. 2, pp. 710–720, Mar. 2007.

[11] Y. Chen, M. Alouini, L. Tang, and F. Khan, "Analytical evaluation of adaptive-modulation-based opportunistic cognitive radio in nakagami-$m$fading channels," *IEEE Trans. Veh. Technol.*, vol. 61, no. 7, pp. 3294–3300, Sep. 2012.

[12] M. Ku, W. Li, Y. Chen, and K. J. R. Liu, "Advances in energy harvesting communications: Past, present, and future challenges," *IEEE Commun. Surveys Tuts.*, vol. 18, no. 2, pp. 1384–1412, Second quarter 2016.

[13] C. L. I, C. Rowell, S. Han, Z. Xu, G. Li, and Z. Pan, "Toward green and soft: A 5G perspective," *IEEE Commun. Mag.*, vol. 52, no. 2, pp. 66–73, Feb. 2014.

[14] S. Park and D. Hong, "Optimal spectrum access for energy harvesting cognitive radio networks," *IEEE Trans. Wireless Commun.*, vol. 12, no. 12, pp. 6166–6179, Dec. 2013.

[15] ——, "Achievable throughput of energy harvesting cognitive radio networks," *IEEE Trans. Wireless Commun.*, vol. 13, no. 2, pp. 1010–1022, Feb. 2014.

[16] J. Pradha, S. S. Kalamkar, and A. Banerjee, "Energy harvesting cognitive radio with channel-aware sensing strategy," *IEEE Commun. Lett.*, vol. 18, no. 7, pp. 1171–1174, July 2014.

[17] Pratibha, K. H. Li, and K. C. Teh, "Optimal spectrum access and energy supply for cognitive radio systems with opportunistic RF energy harvesting," *IEEE Trans. Veh. Technol.*, vol. 66, no. 8, pp. 7114–7122, Aug. 2017.

[18] A. Bhowmick, K. Yadav, S. D. Roy, and S. Kundu, "Throughput of an energy harvesting cognitive radio network based on prediction of primary user," *IEEE Trans. Veh. Technol.*, vol. 66, no. 9, pp. 8119–8128, Sep. 2017.

[19] N. Pappas, J. Jeon, A. Ephremides, and A. Traganitis, "Optimal utilization of a cognitive shared channel with a rechargeable primary source node," *IEEE J. Commun. Netw.*, vol. 14, no. 2, pp. 162–168, Apr. 2012.

[20] R. Duan, M. Elmusrati, and R. Virrankoski, "Stable transmission for a cognitive-shared channel with rechargeable transmitters," in *Proc. IEEE ICC*, Ottawa, Canada, June 2012, pp. 4632–4636.

[21] A. E. Shafie, M. Ashour, T. Khattab, and A. Mohamed, "On spectrum sharing between energy harvesting cognitive radio users and primary users," in *Proc. Int. Conf. Comput. Netw. Commun. (ICNC)*, Garden Grove, CA, USA, Feb 2015, pp. 214–220.

[22] M. A. Abd-Elmagid, T. ElBatt, K. G. Seddik, and O. Ercetin, "Stable throughput of cooperative cognitive networks with energy harvesting: Finite relay buffer and finite battery capacity," *IEEE Trans. Cogn. Commun. Netw.*, vol. 4, no. 4, pp. 704–718, Dec. 2018.

[23] S. Lee, R. Zhang, and K. Huang, "Opportunistic wireless energy harvesting in cognitive radio networks," *IEEE Trans. Wireless Commun.*, vol. 12, no. 9, pp. 4788–4799, Sep. 2013.

[24] E. Boshkovska, D. W. K. Ng, N. Zlatanov, and R. Schober, "Practical non-linear energy harvesting model and resource allocation for SWIPT systems," *IEEE Commun. Lett.*, vol. 19, no. 12, pp. 2082–2085, Dec. 2015.

[25] Q. Zhao, L. Tong, A. Swami, and Y. Chen, "Decentralized cognitive MAC for opportunistic spectrum access in ad hoc networks: A POMDP framework," *IEEE J. Sel. Areas Commun.*, vol. 25, no. 3, pp. 589–600, Apr. 2007.

[26] K. W. Choi and E. Hossain, "Opportunistic access to spectrum holes between packet bursts: A learning-based approach," *IEEE Trans. Wireless Commun.*, vol. 10, no. 8, pp. 2497–2509, Aug. 2011.

[27] S. Huang, X. Liu, and Z. Ding, "Opportunistic spectrum access in cognitive radio networks," in *Proc. IEEE INFOCOM*, Phoenix, AZ, USA, Apr. 2008, pp. 1427–1435.

[28] H. Holma and A. Toskala, *LTE for UMTS: OFDMA and SC-FDMA based radio access.* Wiley, 2009.

[29] C. Tepedelenlioglu, A. Abdi, G. B. Giannakis, and M. Kaveh, "Estimation of doppler spread and signal strength in mobile communications with applications to handoff and adaptive transmission," *Wireless Commun. Mob. Comput.*, vol. 1, no. 2, pp. 221–242, 2001.

[30] M. Zorzi, R. R. Rao, and L. B. Milstein, "ARQ error control for fading mobile radio channels," *IEEE Trans. Veh. Technol.*, vol. 46, no. 2, pp. 445–455, May 1997.

[31] A. Borhani and M. Pätzold, "Correlation and spectral properties of vehicle-to-vehicle channels in the presence of moving scatterers," *IEEE Trans. Veh. Technol.*, vol. 62, no. 9, pp. 4228–4239, Nov. 2013.

[32] S. De, A. Kawatra, and S. Chatterjee, "On the feasibility of network RF energy operated field sensors," in *Proc. IEEE ICC*, Cape Town, South Africa, May 2010, pp. 1–5.

[33] S. Wagner, R. Couillet, M. Debbah, and D. T. M. Slock, "Large system analysis of linear precoding in correlated MISO broadcast channels under limited feedback," *IEEE Trans. Inf. Theory*, vol. 58, no. 7, pp. 4509–4537, July 2012.

[34] P. S. Khairnar and N. B. Mehta, "Discrete-rate adaptation and selection in energy harvesting wireless systems," *IEEE Trans. Wireless Commun.*, vol. 14, no. 1, pp. 219–229, Jan. 2015.

[35] F. Z. Djiroun and D. Djenouri, "MAC protocols with wake-up radio for wireless sensor networks: A review," *IEEE Commun. Surveys Tuts.*, vol. 19, no. 1, pp. 587–618, Mar. 2017.

[36] J. Guo and X. Zhu, "An improved analytical model for RF-DC conversion efficiency in microwave rectifiers," in *Proc. IEEE MTT-S Int. Microw. Symp. Dig.*, Montreal, QC, Canada, June 2012, pp. 1–3.

[37] M. Zorzi and R. R. Rao, "Error control and energy consumption in communications for nomadic computing," *IEEE Trans. Comput.*, vol. 46, no. 3, pp. 279–289, Mar. 1997.

[38] F. Meshkati, H. V. Poor, and S. C. Schwartz, "Energy-efficient resource allocation in wireless networks," *IEEE Signal Process. Mag.*, vol. 24, no. 3, pp. 58–68, May 2007.

[39] C. Xu, M. Zheng, W. Liang, H. Yu, and Y. Liang, "End-to-end throughput maximization for underlay multi-hop cognitive radio networks with RF energy harvesting," *IEEE Trans. Wireless Commun.*, vol. 16, no. 6, pp. 3561–3572, June 2017.

[40] C. Ren, H. Zhang, J. Chen, and C. Tellambura, "Exploiting spectrum access ability for cooperative spectrum harvesting," *IEEE Trans. on Commun.*, vol. 67, no. 3, pp. 1845–1857, Mar. 2019.

[41] S. Agarwal and S. De, "eDSA: Energy-efficient dynamic spectrum access protocols for cognitive radio networks," *IEEE Trans. Mobile Comput.*, vol. 15, no. 12, pp. 3057–3071, Dec. 2016.

[42] S. Maleki, A. Pandharipande, and G. Leus, "Energy-efficient distributed spectrum sensing for cognitive sensor networks," *IEEE Sensors J.*, vol. 11, no. 3, pp. 565–573, Mar. 2011.

[43] "Panasonic BK120AA Datasheet," [Online]. Available: https://na.industrial.panasonic.com/sites/default/pidsa/files/downloads/files/panasonic-bk120aa-datasheet.pdf (Access date: Sep. 2018).

[44] A. M. Koushik, F. Hu, and S. Kumar, "Intelligent spectrum management based on transfer actor-critic learning for rateless transmissions in cognitive radio networks," *IEEE Trans. Mobile Comput.*, vol. 17, no. 5, pp. 1204–1215, May 2018.

[45] A. Goldsmith, *Wireless Communications*. Cambridge University Press, 2005.

[46] S. L. Cotton, "Second-order statistics of $\kappa - \mu$ shadowed fading channels," *IEEE Trans. Veh. Technol.*, vol. 65, no. 10, pp. 8715–8720, Oct. 2016.

[47] P. Mukherjee, D. Mishra, and S. De, "Exploiting temporal correlation in wireless channel for energy-efficient communication," *IEEE Trans. Green Comm. and Networking*, vol. 1, no. 4, pp. 381–394, Dec. 2017.

[48] W. C. Horrace, "Some results on the multivariate truncated normal distribution," *Journal of Multivariate Analysis*, vol. 94, no. 1, pp. 209–221, 2005.

[49] R. K. Mungara, G. George, and A. Lozano, "Overhead and spectral efficiency of pilot-assisted interference alignment in time-selective fading channels," *IEEE Trans. Wireless Commun.*, vol. 13, no. 9, pp. 4884–4895, Sep. 2014.